

Accounts

High Resolution Spectroscopy and Zeeman Effect of the $S_1 \leftarrow S_0$ Transition of Benzene and Naphthalene

Hajime Katô,*[1] Masaaki Baba,[2] and Shunji Kasahara[1]

[1]Molecular Photoscience Research Center, Kobe University, Kobe 657-8501

[2]Division of Chemistry, Graduate School of Science, Kyoto University, Kyoto 606-8502

Received May 11, 2006; E-mail: h-kato@kobe-u.ac.jp

We measured Zeeman effects for rotationally resolved spectra of several low-lying vibrational bands of the $S_1 \leftarrow S_0$ transition of benzene and naphthalene. We demonstrated that for both benzene and naphthalene (i) Zeeman splittings of the rotational lines were caused by a magnetic moment of the S_1 state, and (ii) the magnetic moment lies perpendicular to the molecular plane and originates from an electronic angular momentum induced by *J*–*L* coupling between the S_1 and S_2 states. We found from the Zeeman spectra that the rotational levels of the S_1 state are not mixed with a triplet state, and all the perturbing levels were found to be a singlet state. Coupling to a triplet state was shown not to be responsible for nonradiative relaxation. Accordingly, intersystem crossing is not the dominant nonradiative process at low-lying vibrational states, and the main nonradiative process is presumed to be internal conversion.

1. Introduction

Nonradiative electronic relaxation of organic molecules is a fundamental and important process for studying the chemical dynamics.[1–5] Terminologies intersystem crossing (ISC) and internal conversion (IC) are used to describe radiationless transitions between singlet and triplet states and between electronic states of the same spin multiplicity, respectively, in the time dependent picture. Intersystem mixing and internal mixing are used, respectively, in the stationary state picture.[1] Benzene is a prototypical system in a wide class of aromatic molecules. Extensive studies of the vibrational state dependence of fluorescence lifetimes and quantum yields have been reported.[6–10] The significant nonradiative process was reported to be the $S_1{}^1B_{2u} \rightarrow T_1{}^3B_{1u}$ ISC to account for radiationless decay of low-lying vibrational levels of the $S_1{}^1B_{2u}$ state. The rotational structure of the $S_1 \leftarrow S_0$ transition was observed to be washed out for excess energy (E_{excess}) higher than 3000 cm^{-1},[11] and the term "channel three" was introduced to describe the nonradiative process, because it was thought that fluorescence and ISC could not account for the phenomenon. "Channel three" was later demonstrated to occur by $S_1{}^1B_{2u} \rightarrow S_0{}^1A_{1g}$ IC via anharmonic and Coriolis couplings in the S_1 state.[12,13]

Naphthalene has also been extensively studied, and the fluorescence lifetimes and quantum yields of naphthalene vapor have been measured as a function of excitation energy.[3,5] The results have been interpreted such that $S_1 \rightarrow T$ ISC was the predominant channel of nonradiative decay at low excess energies in the S_1 state, and the $S_1{}^1B_{1u} \rightarrow S_0{}^1A_g$ IC became increasingly important with increasing excess vibrational energies.[14–16]

Presence of ISC to a triplet state was deduced indirectly by the sensitized emission from biacetyl[15,17] and the sensitized *cis*–*trans* isomerization of 2-butene.[18] Subsequently, the decay of a singlet state excited by a pulsed laser was observed to be biexponential and was analyzed by assuming that the fast component and the slow component were ascribed to singlet and triplet state decay rates, respectively, of the initially populated level.[19,20] However, both components could be ascribed to vibrational levels of short and long lifetimes in the S_1 state because many levels were excited simultaneously.

If the Zeeman effect of rotationally resolved spectrum of the $S_1 \leftarrow S_0$ transition could be measured, direct information on the mixing of a triplet state could be obtained. Recently, we measured Zeeman effects of rotationally resolved spectra of several low-lying vibrational bands of the $S_1 \leftarrow S_0$ transition of benzene and naphthalene.[21–28] In this account, we present the results and analysis of these studies.

2. High-Resolution Zeeman Spectroscopy

The development of a tunable single-frequency laser has enabled high resolution spectroscopy to overcome the resolution limits due to the Doppler effect.[29] Several techniques of Doppler-free high-resolution spectroscopy have been established, and some have been successfully applied to benzene and naphthalene.[30–33] By crossing a laser beam perpendicular to a collimated molecular beam, sub-Doppler high-resolution excitation spectra and Zeeman effects have been measured.[22,27] By counterpropagating laser beams of identical frequency within an optical cavity, Doppler-free two-photon excitation (DFTPE) spectra and Zeeman effects have been measured.[21,23–26,28] In

Published on the web March 13, 2007; doi:10.1246/bcsj.80.456

both experiments, an external magnetic field was applied perpendicular to the propagation vector of the laser beam, which was linearly polarized perpendicular to the magnetic field (σ-pump). Two-photon spectroscopy can be applied to g–g transitions and one-photon spectroscopy to g–u transitions, and these spectroscopy techniques can be used to study states of different symmetries.

When an external magnetic field $\boldsymbol{H}$ is along the space-fixed Z axis, the Hamiltonian of the Zeeman interaction is written as[34]

$$H_Z = -(m_0 D^1_{00} - m_{+1} D^1_{0-1} - m_{-1} D^1_{0+1})H, \tag{1}$$

where m_α is a spherical component of the magnetic moment $\boldsymbol{m}$ and $D^1{}_{\alpha\beta}$ is the rotation matrix of rank 1. For wave functions $|\Gamma\nu JKM\rangle = |\Gamma\rangle|\nu\rangle|JKM\rangle$, where $|\Gamma\rangle$, $|\nu\rangle$, and $|JKM\rangle$ are the wave functions of the electronic part, vibrational part, and rotational part of a symmetric top molecule, respectively, the matrix element of H_Z is expressed as[34]

$$\begin{aligned}
&\langle \Gamma\nu JKM|H_Z|\Gamma\nu JK'M'\rangle \\
&= -\delta_{MM'}H\frac{M}{[J(J+1)]^{1/2}}\left\{\langle\Gamma\nu|m_0|\Gamma\nu\rangle\frac{K}{[J(J+1)]^{1/2}}\delta_{K'K}\right. \\
&\quad - \langle\Gamma\nu|m_{+1}|\Gamma\nu\rangle\left[\frac{(J+K)(J-K+1)}{2J(J+1)}\right]^{1/2}\delta_{K'K-1} \\
&\quad \left. + \langle\Gamma\nu|m_{-1}|\Gamma\nu\rangle\left[\frac{(J-K)(J+K+1)}{2J(J+1)}\right]^{1/2}\delta_{K'K+1}\right\},
\end{aligned} \tag{2}$$

where the quantum numbers M and K are projections of $\boldsymbol{J}$ along the space-fixed Z-axis and the molecule-fixed top axis (z-axis), respectively.

If the magnetic moment of a molecule is along the molecule-fixed z-axis, it is expressed as

$$\begin{aligned}
&\langle \Gamma\nu JKM|H_Z|\Gamma\nu JK'M'\rangle \\
&\quad = -\delta_{MM'}\delta_{K'K}H\langle\Gamma\nu|m_0|\Gamma\nu\rangle\frac{MK}{J(J+1)}.
\end{aligned} \tag{3}$$

The Zeeman energy of a level $\Gamma\nu JK$ has a maximum and minimum at $M = +J$ and $M = -J$. The magnitude of Zeeman splitting (energy spacing between $M = +J$ and $M = -J$ components) of the level $\Gamma\nu JK$ is given by

$$ZS(\Gamma\nu JK) = H\langle\Gamma\nu|m_0|\Gamma\nu\rangle\frac{2K}{J+1}. \tag{4}$$

3. Patterns of Zeeman Spectra

When the excitation light is linearly polarized along the space-fixed X-axis and the electric dipole transition moment of a molecule is perpendicular to the top axis, electric dipole transitions of a symmetric top molecule are allowed for $\Delta J = 0, \pm1$, $\Delta K = \pm1$, and $\Delta M = \pm1$. The P and R lines ($\Delta J = -1$ and $+1$) of one-photon absorption have intensity maxima at $M = \pm J$, and the Zeeman spectra have intensity maxima at high and low energy ends.[22]

The intensity of the DFTPE spectrum is proportional to the intensity of two-photon absorption. Theories of rotational line intensities of two-photon absorption were developed by Metz et al.[35] For excitation by a light linearly polarized along the space-fixed X-axis, the intensity of the ${}^{Q(K)}Q(J)$ line ($\Delta J = 0$, $\Delta K = 0$) is proportional to[21]

$$\begin{aligned}
P^X(f\nu' JKM \leftarrow i\nu'' JKM \quad \text{and} \quad M \pm 2) &= \frac{4}{9}(M_{00} - M_{1-1} - M_{-11})^2 \\
&+ \frac{9(-2J - J^2 + 2J^3 + J^4 + 5M^2 - 2JM^2 - 2J^2M^2 + M^4) + 2(J + J^2 - 3M^2)^2}{18J^2(J+1)^2(2J-1)^2(2J+3)^2}(J + J^2 - 3K^2)^2(2M_{00} + M_{1-1} + M_{-11})^2 \\
&- \frac{4(J + J^2 - 3K^2)(J + J^2 - 3M^2)}{9J(J+1)(2J-1)(2J+3)}(M_{00} - M_{1-1} - M_{-11})(2M_{00} + M_{1-1} + M_{-11}),
\end{aligned} \tag{5}$$

where

$$M_{\lambda\lambda'} = \sum_{m\nu(\neq f\nu', i\nu'')} \langle f\nu'|\mu_{r_\lambda}|m\nu\rangle\langle m\nu|\mu_{r_{\lambda'}}|i\nu''\rangle/(E_m - h\nu). \tag{6}$$

The operator μ_{r_λ} is the spherical component of the transition dipole moment in the molecule-fixed coordinates. The values of $P^X(f\nu' JKM \leftarrow i\nu'' JKM$ and $M \pm 2)$ at $J = 30$ and $K = 30$ are plotted against M for the case of $M_{1-1} + M_{-11} = 0$ in Fig. 1a in units of $|M_{00}|^2$ and for the case of $M_{00} = 0$ in Fig. 1b in units of $|M_{1-1} + M_{-11}|^2$. If $M_{00} \gg M_{1-1} + M_{-11}$, the Zeeman spectrum has an intensity maximum at $M = 0$ and minima at $M = \pm J$. If $M_{1-1} + M_{-11} \gg M_{00}$, the Zeeman spectrum has intensity maxima at $M = \pm J$ and a minimum at $M = 0$.

4. Perturbations

An energy shift from a regular position of a bright (allowed) level and an appearance of transition to a dark (forbidden) level occur by an interaction between bright and dark levels. This perturbation becomes appreciable when levels which satisfy the selection rule of an interaction are close in energy. The energies E_+ and E_- of two levels coupled through an interaction matrix element, $V_{bd} = \langle b|V|d\rangle$, are given by

$$E_\pm = \frac{E_b + E_d}{2} \pm \frac{1}{2}[(E_b - E_d)^2 + 4{V_{bd}}^2]^{1/2}, \tag{7}$$

where E_b and E_d are energies of bright and dark levels, respectively, in the absence of perturbation. From Eq. 7, we have $E_+ + E_- = E_b + E_d$. The energy E_d can be evaluated from observed values of E_+ and E_- and the value of E_b ($=E_{\text{cal}}$) calculated by the molecular constants, which are determined from unperturbed lines. Then, the value of V_{bd} can be evaluated by Eq. 7. By studying the J and K dependence of V_{bd}, the character of interaction can be explored.

5. Studies on Benzene

We measured the DFTPE spectra and Zeeman effects of the $1_0{}^1 14_0{}^1$ ($E_{\text{excess}} = 2492\,\text{cm}^{-1}$) and $1_0{}^2 14_0{}^1$ ($E_{\text{excess}} = 3412\,\text{cm}^{-1}$) bands of C_6H_6, and the $14_0{}^1$ ($E_{\text{excess}} = 1568\,\text{cm}^{-1}$) and $1_0{}^1 14_0{}^1$ ($E_{\text{excess}} = 2446\,\text{cm}^{-1}$) bands of C_6D_6 of the $S_1{}^1B_{2u} \leftarrow$

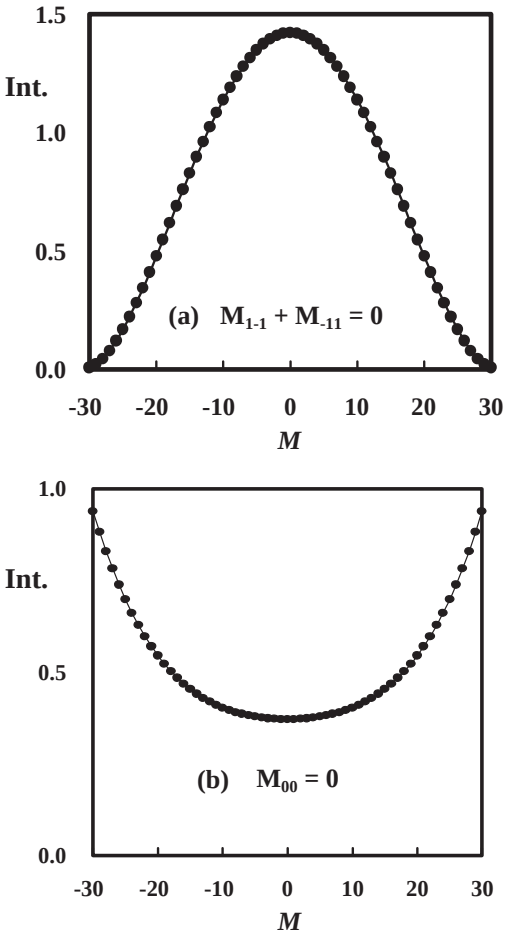

Fig. 1. Relative intensity of the DFTPE Zeeman spectrum of the $^{Q(30)}Q(30)$ line under the σ-pump (Ref. 21).

$S_0{}^1A_{1g}$ transition.[21,23–25] Only $^{Q(K)}Q(J)$ lines were observed, and the rotational lines were fully resolved. Part of the spectrum of the $1_0{}^1 14_0{}^1$ band of C_6H_6 is shown in Fig. 2. The rotational levels ($J = 25$, $K = 21$) and ($J = 26$, $K = 23$) of the $S_1{}^1B_{2u}$ ($\nu_1 = 1$, $\nu_{14} = 1$) state are perturbed. We found the magnitude of Zeeman splittings of bright and dark lines (25_{21} and $d25_{21}$ lines, 26_{23} and $d26_{23}$ lines in Fig. 2) to be approximately the same. This demonstrates that the perturbing level is a singlet state.

The Zeeman spectra of $^{Q(K=J)}Q(J)$ lines (Examples are $^{Q(29)}Q(29)$ line in Fig. 2, $^{Q(30)}Q(30)$ line in Fig. 3) were observed to have intensity maxima at $M = \pm J$ and minimum at $M = 0$. The observed Zeeman patterns were similar to those calculated for $M_{00} = 0$, but were different from that of $M_{1-1} + M_{-11} = 0$ (Fig. 1). Accordingly, $M_{1-1} + M_{-11} \gg M_{00}$.

The K dependence of the Zeeman spectra of $^{Q(K)}Q(J = 30)$ lines of the $1_0{}^1 14_0{}^1$ band of C_6H_6 at $H = 1.2$ T is shown in Fig. 3. The Zeeman splittings of $^{Q(K)}Q(J)$ lines were observed to increase as K increases for a given J, and is coincident with Eq. 4. Accordingly, the magnetic moment of the level, which splits by the Zeeman effect, is along the molecule-fixed z-axis.

The magnetic moment along the z-axis (m_z) has a symmetry of A_{2g} in the point group D_{6h}. If the ground state $S_0{}^1A_{1g}$ is mixed with a $^1A_{2g}$ state, the mixed state can have a magnetic moment along the molecule-fixed z-axis. However, there is no $^1A_{2g}$ state in the low energy region.[4] If the excited state $S_1{}^1B_{2u}$ is mixed with the $S_2{}^1B_{1u}$ state, the mixed state can have non-vanishing magnetic moment through the matrix element $\langle S_1{}^1B_{2u}|m_z|S_2{}^1B_{1u}\rangle$, where $m_z = -\mu_B L_z$, in which μ_B is the Bohr magneton and L_z is the z-component of an orbital angular momentum of electrons. The $S_2{}^1B_{1u}$ state can be mixed with the $S_1{}^1B_{2u}$ state by the J–L coupling term $-2CJ_zL_z$, where C is the rotational constant along the z-axis (c-axis). The elec-

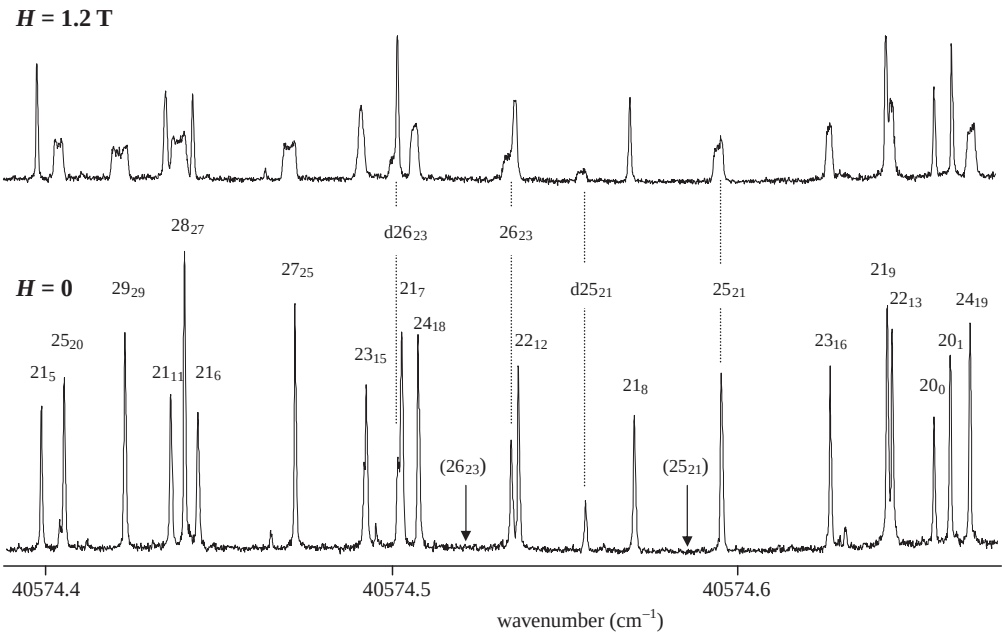

Fig. 2. Part of the DFTPE spectra of the $1_0{}^1 14_0{}^1$ band of C_6H_6 (1 Torr) at magnetic fields $H = 0$ and 1.2 T (Ref. 21). Assignments of $^{Q(K)}Q(J)$ lines are indicated above the lines as J_K. The energies of the 25_{21} and 26_{23} lines calculated from the molecular constants are shown by arrows (↓). The "dark" lines allowed via interaction with 25_{21} and 26_{23} lines are indicated as $d25_{21}$ and $d26_{23}$, respectively.

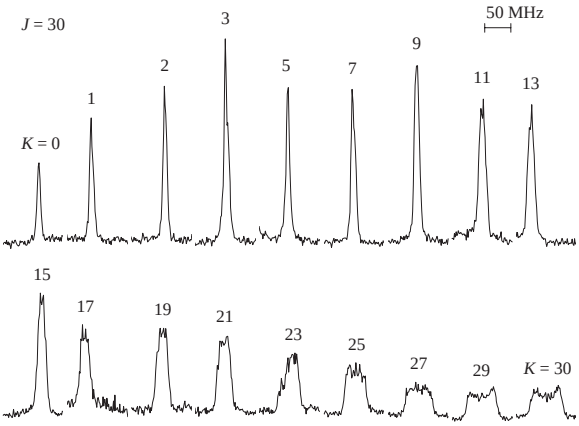

Fig. 3. K dependence of DFTPE Zeeman spectra of the $^{Q(K)}Q(J = 30)$ lines of the $1_0^1 14_0^1$ band of C_6H_6 at $H = 1.2\,\mathrm{T}$ (Ref. 21).

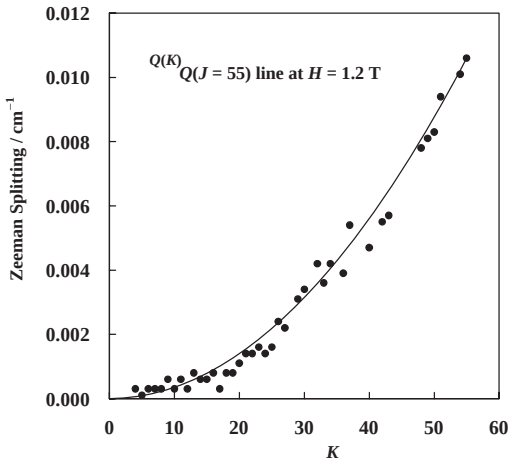

Fig. 4. K dependence of Zeeman splittings of the $^{Q(K)}Q(J = 55)$ lines of the $1_0^1 14_0^1$ band of C_6H_6 at $H = 1.2\,\mathrm{T}$ (Ref. 25). Zeeman splitting of the $^{Q(55)}Q(55)$ line was $0.0106\,\mathrm{cm^{-1}}$, and the solid line is a function $0.0106K^2/55^2$ in units of $\mathrm{cm^{-1}}$.

tronic part of the mixed wave function is expressed by the first-order perturbation theory as

$$|S_1{}^1B_{2u}\rangle - 2CJ_z \frac{\langle S_2{}^1B_{1u}|L_z|S_1{}^1B_{2u}\rangle}{E(S_1) - E(S_2)} |S_2{}^1B_{1u}\rangle. \quad (8)$$

By substituting Eq. 8 into Eq. 4, the magnitude of Zeeman splitting of the mixed $S_1{}^1B_{2u}$ (v, J, K) level is given by

$$ZS(^1B_{2u}vJK) = \frac{8CK^2}{J+1} \frac{|\langle S_2{}^1B_{1u}|L_z|S_1{}^1B_{2u}\rangle|^2}{E(S_2) - E(S_1)} \mu_B H. \quad (9)$$

Zeeman splitting of the $^{Q(K)}Q(J)$ line of a given J was observed to increase in proportion to K^2 (Fig. 4).[25] The Zeeman splitting of the $^{Q(K=J)}Q(J)$ line was observed to increase in proportion to J (Fig. 5).[21] Eq. 9 is consistent with these observations. The matrix element $\langle S_2{}^1B_{1u}|L_z|S_1{}^1B_{2u}\rangle$ was evaluated to be $-1.729\hbar$ from simple molecular orbitals.[22] By using this value with $C = 0.0906\,\mathrm{cm^{-1}}$, $E(S_1) = 38086\,\mathrm{cm^{-1}}$, and $E(S_2) = 46500\,\mathrm{cm^{-1}}$, we calculated Zeeman splitting of the C_6H_6 $S_1{}^1B_{2u}$ ($\nu_1 = 1$, $\nu_{14} = 1$, $J = 55$, $K = 55$) level at

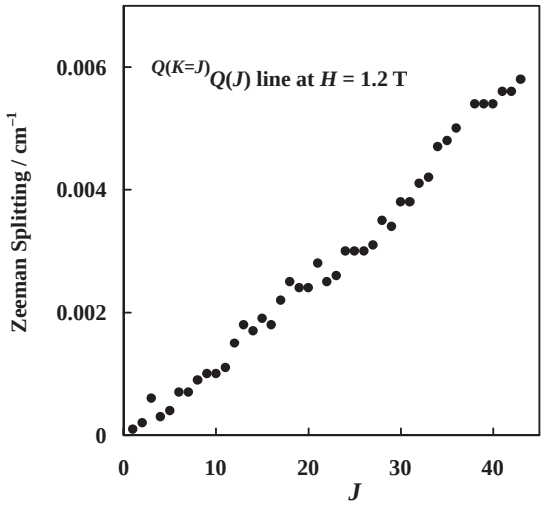

Fig. 5. J dependence of Zeeman splittings of the $^{Q(K=J)}Q(J)$ lines of the $1_0^1 14_0^1$ band of C_6H_6 at $H = 1.2\,\mathrm{T}$ (Ref. 21).

$H = 1.2\,\mathrm{T}$ by Eq. 9 to be $0.0078\,\mathrm{cm^{-1}}$, which is in accordance with the observed value of $0.0106\,\mathrm{cm^{-1}}$.[25] Similar results were obtained for Zeeman splittings of the $^{Q(K=J)}Q(J)$ lines of C_6D_6.[24] Accordingly, it was concluded that (i) Zeeman splittings of the rotational lines in the $1_0^1 14_0^1$ band of C_6H_6 and the 14_0^1 and $1_0^1 14_0^1$ bands of C_6D_6 are caused by a magnetic moment of the $S_1{}^1B_{2u}$ state, and (ii) the magnetic moment lies perpendicular to the molecular plane and originates from an electronic angular momentum induced by the J–L coupling between the $S_1{}^1B_{2u}$ and $S_2{}^1B_{1u}$ states.

Sub-Doppler high-resolution excitation spectra and the Zeeman effects of the 6_0^1 ($E_{\mathrm{excess}} = 520\,\mathrm{cm^{-1}}$), $1_0^1 6_0^1$ ($E_{\mathrm{excess}} = 1444\,\mathrm{cm^{-1}}$), and $1_0^2 6_0^1$ ($E_{\mathrm{excess}} = 2366\,\mathrm{cm^{-1}}$) bands of the $S_1 \leftarrow S_0$ transition of C_6H_6 were measured by crossing a laser beam perpendicular to a collimated molecular beam.[22] For all of these bands, the Zeeman splittings of the lines of a given J were observed to increase with K, and those of $K = J$ lines were observed to increase linearly with J. The magnitude of Zeeman splitting of the $S_1{}^1B_{2u}$ ($J = 25$, $K = 25$) level in the vibrational states 6^1, $1^1 6^1$, and $1^2 6^1$ was observed to be $0.0033 \pm 0.0007\,\mathrm{cm^{-1}}$ at $H = 1.1\,\mathrm{T}$. By using $\langle S_2{}^1B_{1u}|L_z|S_1{}^1B_{2u}\rangle = -1.729\hbar$, $C = 0.09086\,\mathrm{cm^{-1}}$, $E(S_1) = 38086\,\mathrm{cm^{-1}}$, and $E(S_2) = 46500\,\mathrm{cm^{-1}}$, the Zeeman splitting of the $S_1{}^1B_{2u}$ ($\nu_1 = 1$, $\nu_6 = 1$, $J = 25$, $K = 25$) level at $H = 1.1\,\mathrm{T}$ was calculated by Eq. 9 to be $0.0032\,\mathrm{cm^{-1}}$, which is in accordance with the observed value. Therefore, the Zeeman splittings in the 6^1, $1^1 6^1$, and $1^2 6^1$ states are also identified as originating from the electronic orbital angular momentum caused by a mixing of the $S_1{}^1B_{2u}$ and $S_2{}^1B_{1u}$ states via J–L coupling.

The nonradiative decay of benzene excited to low vibrational levels of the S_1 state was attributed to the $S_1 \rightarrow T_1$ ISC.[8] If true, the eigenfunction of the full molecular Hamiltonian of a rotationally resolved excited level $S_1{}^1B_{2u}$ ($vJKM$) is expressed as

$$C^S|JKM\rangle|v\rangle|S_1{}^1B_{2u}\rangle + \sum_{m,n} C_{mn}^T|J_m K_m M_m\rangle|v_n\rangle|T_1{}^3B_{1u}\rangle, \quad (10)$$

where C^S and $C_{mn}{}^T$ are the coefficients. Eq. 10 holds even

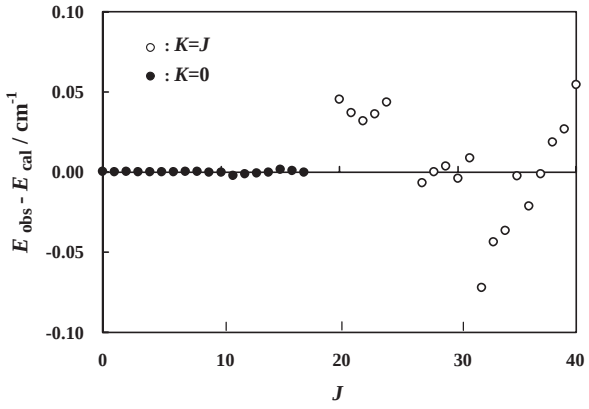

Fig. 6. The difference $E_{obs} - E_{cal}$ for all assigned lines of $1_0^2 14_0^1$ band of C_6H_6 is plotted by a closed circle (●) for the ${}^{Q(0)}Q(J)$ line and by an open circle (○) for the ${}^{Q(K=J)}Q(J)$ line (Ref. 25).

if a level in the S_1 state is coupled with many rovibrational levels in the T_1 state. The quantum yield of the $1_0^1 6_0^1$ band has been reported to be 0.25.[6] If nonradiative decay occurs by the $S_1 \rightarrow T_1$ ISC, the matrix element $\langle S_1{}^1B_{2u}(1^1 6^1 JKM)|m_z|S_1{}^1B_{2u}(1^1 6^1 JKM)\rangle$ can be evaluated approximately by $0.75\langle T_1{}^3B_{1u}|m_z|T_1{}^3B_{1u}\rangle$. Contribution from an electron spin angular momentum $-g_e S_z \mu_B$ is predominant in the matrix element $\langle T_1{}^3B_{1u}|m_z|T_1{}^3B_{1u}\rangle$, where g_e is the g value for an electron and S_z is the z component of an electron spin angular momentum $\boldsymbol{S}$. The resulting Zeeman splittings are different from the observed ones in both the pattern and the magnitude. Therefore, rotationally resolved levels of the S_1 state are demonstrated not to be mixed with a triplet state.

DFTPE spectra of the $1_0^2 14_0^1$ band of C_6H_6, which lies in the region of "channel three," were first measured by Riedle et al.[36,37] Only rotational lines of $K = 0$ were observed near the band origin, and lines of $K = J$ were observed to be dominant in the red region. Recently, Baek et al.[25] measured the DFTPE spectra and Zeeman effects. Zeeman splittings of the $K = 0$ lines were observed to be small, and those of the $K = J$ lines were observed to increase in proportion to J. The difference between the observed transition energy (E_{obs}) and the energy calculated (E_{cal}) from the molecular constants is plotted in Fig. 6 for all of the assigned lines. Strong agreement was observed for ${}^{Q(0)}Q(J)$ lines, whereas poor agreement was observed for ${}^{Q(K=J)}Q(J)$ lines. These results support the assignments and conclusions stated in previous studies[36,37] that the spectrum near the band origin is broadened through parallel Coriolis interaction (which is proportional to K with the selection rule $\Delta K = 0$ and it is zero for a level of $K = 0$), and the spectrum in the red region is broadened through perpendicular Coriolis interaction, which is proportional to $[J(J+1) - K(K \pm 1)]^{1/2}$ with the selection rule $\Delta K = \pm 1$ and is nonzero even at $K = J$ for $\Delta K = -1$.

At high J levels of the $S_1{}^1B_{2u}$ ($\nu_1 = 1$, $\nu_{14} = 1$) state of C_6H_6, of which excess energy is isoenergetic with the one of low J levels of the $S_1{}^1B_{2u}$ ($\nu_1 = 2$, $\nu_{14} = 1$) state of C_6H_6, the density of perturbation was observed to be high, but line broadening was not observed. This demonstrates that line broadening depends not only on the excess energy, but also on the vibrational character of the excited state. This is consistent with the conclusion[38] that the rate of the $S_1 \rightarrow S_0$ IC depends on the magnitude of nonadiabatic interaction between isoenergetic vibrational levels $\nu(S_1)$ in the S_1 state and $\nu(S_0)$ in the S_0 state.

Zeeman splittings, which could be attributed to the perturbation with a triplet state, were not observed in the $1_0^1 14_0^1$, $1_0^2 14_0^1$, 6_0^1, $1_0^1 6_0^1$, and $1_0^2 6_0^1$ bands of C_6H_6 and the 14_0^1 and $1_0^1 14_0^1$ bands of C_6D_6. Therefore, we conclude that nonradiative decay of an isolated benzene excited to low vibronic levels in the S_1 state does not occur through ISC. Nonradiative decay of low vibronic levels is presumed, instead, to occur through $S_1 \rightarrow S_0$ IC as was concluded for the "channel three" decay. The nonradiative decay rate in the region of low excess energy is smaller than that in the "channel three" region.

Decay to the highly excited vibronic levels in the S_0 state and the $T_n \leftarrow T_1$ absorption were observed when benzene at 20 Torr was excited by a light of 40258 cm^{-1} of the KrF laser.[39] The vibronically highly excited benzene in the S_0 state is produced through the $S_1 \rightarrow S_0$ IC. Under sufficiently high pressure, benzene in the T_1 state is presumably produced through collisions of benzene relaxed to high vibronic levels in the S_0 state or $\nu = 0$ level in the S_1 state. If Zeeman spectra of the S_1 ($\nu = 0$) $\leftarrow S_0$ transition and the $T_1 \leftarrow S_0$ transition could be measured, this problem would be solved. Improvement in the sensitivity of our equipment is necessary for further studies.

6. Studies on Naphthalene

Naphthalene has D_{2h} symmetry. The asymmetry parameter is -0.69, and naphthalene is a limiting case of a prolate symmetric top. Unlike previous studies,[40] we chose the figure axis (a-axis) as the z-axis and the y-axis as normal to the molecular plane (c-axis). The vibrational modes were numbered according to Herzberg[41] and can be found in Table 1 of Joo et al.[27] The fluorescence lifetime and quantum yield of an isolated naphthalene molecule were measured, and the nonradiative processes in the region of low excess vibrational energies were assumed to be the $S_1 \rightarrow T_i$ ($i = 2$ or 3) ISC.[5,14–16] It should be noted that the ISC yields were determined indirectly from excitation spectra of biacetyl phosphorescence.[15]

The rotationally resolved DFTPE spectra and Zeeman effects of the $S_1{}^1B_{1u}$ ($\nu_{21} = 1$) $\leftarrow S_0{}^1A_g$ ($\nu = 0$) transition were measured for $C_{10}H_8$ and $C_{10}D_8$.[26,28] For an excitation by linearly polarized photons, only ${}^{Q(K_a)}Q(J)_{K_a K_c}$ lines were observed, where the quantum numbers K_a and K_c are projections of the angular momentum $\boldsymbol{J}$ along the a- and c-axes, respectively. The vibrational excess energies of the $S_1{}^1B_{1u}$ ($\nu_{21} = 1$) level are 1559.452 and 1555.333 cm^{-1} in $C_{10}H_8$ and $C_{10}D_8$, respectively. In the spectrum of $C_{10}H_8$, we identified perturbation originating from a parallel Coriolis interaction, whereas in the spectrum of $C_{10}D_8$, we identified perturbation originating from a perpendicular Coriolis interaction.

DFTPE spectra at magnetic fields $H = 0$ and 0.5 T were measured alternately for each scan of 0.5 cm^{-1} in length.[26] Part of the spectrum of $C_{10}H_8$ is shown in Fig. 7. In both $C_{10}H_8$ and $C_{10}D_8$, the Zeeman splittings of the ${}^{Q(K_a)}Q(J)_{K_a K_c}$ lines of a given J were observed to increase in proportion to $K_c{}^2$, and the Zeeman splittings of the $K_c = J$ lines were ob-

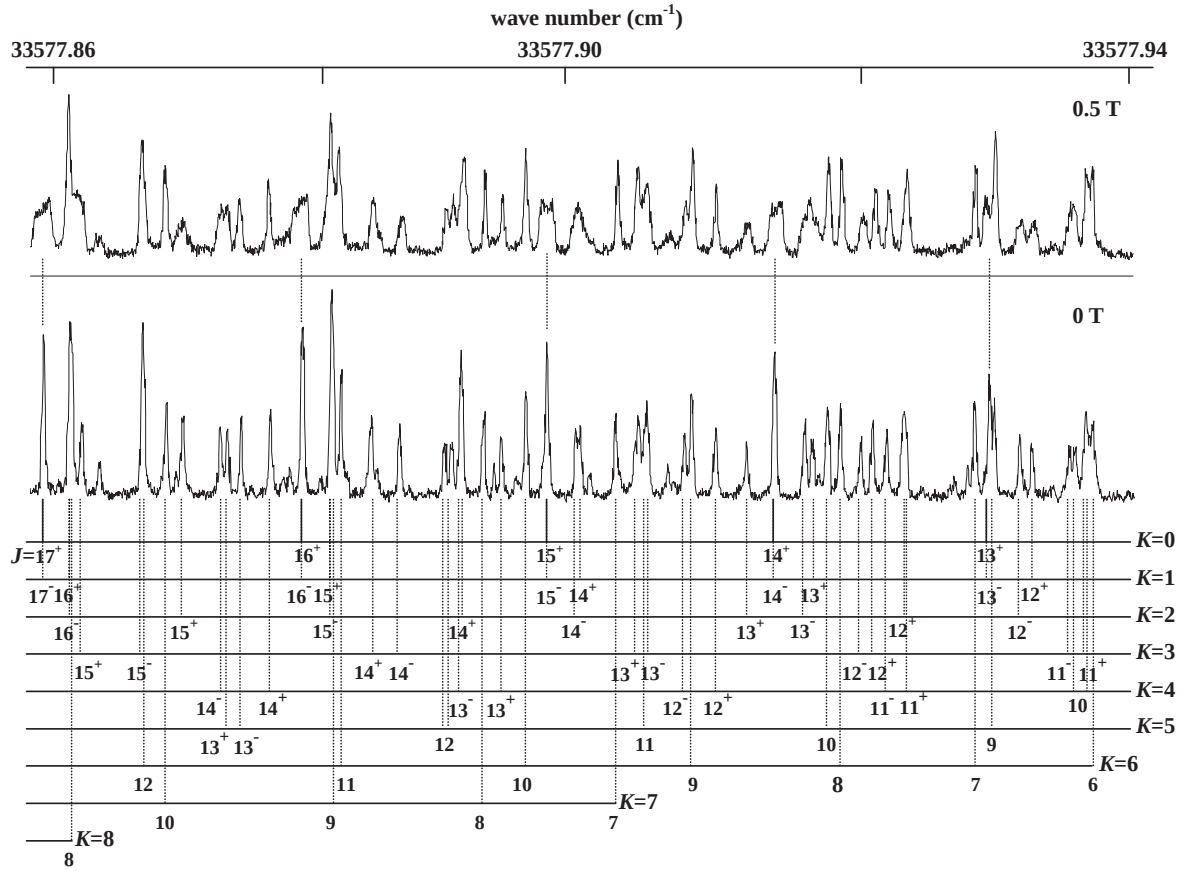

Fig. 7. Part of the DFTPE spectra of $C_{10}H_8$ (0.1 Torr) at magnetic fields $H = 0$ and 0.5 T (Ref. 26). Assignments of ${}^{Q(K_a)}Q(J)_{K_aK_c}$ lines are shown below the spectrum. Lines labeled by J^+ and J^- for each K ($=K_a$) are lines of $K_a + K_c = J$ and $K_a + K_c = J + 1$, respectively. When J^+ and J^- lines are degenerate, J is used solely.

served to increase in proportion to J, when J is large. These tendencies are similar to those observed in benzene. Using a similar analysis as that performed for benzene, these trends and the magnitude of Zeeman splittings have been explained.[28] Accordingly, we conclude that (i) Zeeman splittings are induced by a magnetic moment of the $S_1{}^1B_{1u}$ state, and (ii) the magnetic moment lies perpendicular to the molecular plane and originates from an electronic angular momentum induced by the J–L coupling between $S_1{}^1B_{1u}$ and $S_2{}^1B_{3u}$ states.

The emission spectra from the lowest triplet state (phosphorescence) of gaseous naphthalene-d_8 and -h_8 were observed by Gattermann and Stockburger.[15] They suggested that the $S_1 \rightarrow T_i$ ISC is the only pathway of nonradiative transition for low rovibronic levels in the $S_1{}^1B_{1u}$ state. The collision-free quantum yield of fluorescence from a level in $C_{10}D_8$ of the vibrational excess energy of 1591 cm^{-1}, which is close in energy to the excess energy of the $S_1{}^1B_{1u}$ ($\nu_{21} = 1$) level of $C_{10}D_8$, was reported to be 0.235.[16] If the rest of decay occurs through the $S_1 \rightarrow T_i$ ISC, the magnetic moment $\langle S_1{}^1B_{1u}|m_z|S_1{}^1B_{1u}\rangle$ can be evaluated approximately by $0.765\langle T_i|m_z|T_i\rangle$. In this case, Zeeman splitting of the rotationally resolved line arises predominantly from an electron spin angular momentum, and the resulting Zeeman splittings are much larger than those observed. It is clear that the rotationally resolved levels of the $S_1{}^1B_{1u}$ state are not mixed with a triplet state. Accordingly, we concluded that nonradiative decay of an isolated naphthalene molecule excited to the $S_1{}^1B_{1u}$ ($\nu_{21} = 1$) state does not occur through the $S_1 \rightarrow T_i$ ISC. Coriolis interactions were observed in the $S_1{}^1B_{1u}$ ($\nu_{21} = 1$) state of naphthalene-d_8 and -h_8. Since ISC is not the source of the low fluorescence quantum yield, the $S_1 \rightarrow S_0$ IC was presumed to be the source. The IC should be enhanced by anharmonic and Coriolis interactions with vibronic levels in the S_1 state, which couple strongly with the highly excited vibronic levels in the S_0 state.

Ashpole, Formosinho, and Porter[42] reported that the triplet yield of naphthalene decreased as the total gas pressure was decreased, approaching zero at zero pressure. Schröder, Neusser, and Schlag[43] measured the $T^* \leftarrow T_1$ absorption spectra shortly after the $S_1 \leftarrow S_0$ excitation. Naphthalene in the T_1 state is presumably produced through collisions of naphthalene relaxed to high vibronic levels in the S_0 state or $\nu = 0$ level in the S_1 state. More extensive studies are necessary to solve this problem.

7. Concluding Remarks

We measured rotationally resolved spectra and the Zeeman effects of several low-lying vibrational bands of the $S_1 \leftarrow S_0$ transition of benzene and naphthalene. Almost all the observed lines near the band origins could be assigned. Perturbations originating from a perpendicular Coriolis interaction, a parallel Coriolis interaction, and an anharmonic resonance interaction were identified. The density of perturbed lines were found to

increase, in general, as the rotational and vibrational excess energy increases.

Zeeman splitting in the benzene spectrum was observed to increase in proportion to K^2 for a given J, and that of the $K = J$ line was observed to increase in proportion to J. Zeeman splitting in the naphthalene spectrum was observed to increase in proportion to ${K_c}^2$ for a given J, and that of the $K_c = J$ line was observed to increase in proportion to J. From this, we concluded that for both benzene and naphthalene (i) Zeeman splittings of the rotational lines were caused by a magnetic moment of the S_1 state, and (ii) the magnetic moment lies perpendicular to the molecular plane and originates from an electronic angular momentum induced by J–L coupling between the S_1 and S_2 states.

It is clear from the Zeeman spectra that rotationally resolved levels of the S_1 state are not mixed with a triplet state, and all the perturbing levels are a singlet state. We observed no coupling to a triplet state. In the stationary state picture, intersystem mixing was demonstrated not to exist in the S_1 states of both benzene and naphthalene. Therefore, ISC could not be the dominant nonradiative process at low lying vibrational states, and the main nonradiative process is presumed to be IC. The $S_1 \rightarrow S_0$ IC becomes efficient when the optically excited vibronic levels mix with the background levels in the S_1 state, which couple strongly with the highly excited vibronic levels in the S_0 state.

For decades, observation of Zeeman splitting has been limited to diatomic molecules or paramagnetic molecules. However, with improving spectral resolution, it is now possible to measure Zeeman effects for most molecules. Zeeman spectra yield information regarding the magnetic moment and coupling between the excited states, while facilitating the assignment of spectral lines.

This work is supported by a Grant-in-Aid of JSPS and a grant for the Future Program of JSPS.

References

1 B. R. Henry, M. Kasha, *Annu. Rev. Phys. Chem.* **1968**, *19*, 161.
2 C. S. Parmenter, *Adv. Chem. Phys.* **1972**, *22*, 365.
3 P. Avouris, W. M. Gelbart, M. A. El-Sayed, *Chem. Rev.* **1977**, *77*, 793.
4 L. D. Ziegler, B. S. Hudson, *Excited States* **1982**, *5*, 41.
5 E. C. Lim, *Adv. Photochem.* **1997**, *23*, 165.
6 C. S. Parmenter, M. W. Schuyler, *Chem. Phys. Lett.* **1970**, *6*, 339.
7 W. R. Ware, B. K. Selinger, C. S. Parmenter, M. W. Schuyler, *Chem. Phys. Lett.* **1970**, *6*, 342.
8 W. M. Gelbart, K. G. Spears, K. F. Freed, J. Jortner, S. A. Rice, *Chem. Phys. Lett.* **1970**, *6*, 345.
9 K. G. Spears, S. A. Rice, *J. Chem. Phys.* **1971**, *55*, 5561.
10 T. A. Stephenson, S. A. Rice, *J. Chem. Phys.* **1984**, *81*, 1073.
11 J. H. Callomon, J. E. Parkin, R. Lopez-Delgado, *Chem. Phys. Lett.* **1972**, *13*, 125.
12 E. Riedle, T. Weber, U. Schubert, H. J. Neusser, E. W. Schlag, *J. Chem. Phys.* **1990**, *93*, 967.
13 A. Helman, R. A. Marcus, *J. Chem. Phys.* **1993**, *99*, 5011.
14 J. C. Hsieh, C. S. Huang, E. C. Lim, *J. Chem. Phys.* **1974**, *60*, 4345.
15 H. Gattermann, M. Stockburger, *J. Chem. Phys.* **1975**, *63*, 4541.
16 F. M. Behlen, S. A. Rice, *J. Chem. Phys.* **1981**, *75*, 5672.
17 H. Ishikawa, W. A. Noyes, Jr., *J. Chem. Phys.* **1962**, *37*, 583.
18 R. B. Cundall, F. J. Fletcher, D. G. Milne, *Trans. Faraday Soc.* **1964**, *60*, 1146.
19 M. A. Duncan, T. G. Dietz, M. G. Liverman, R. E. Smalley, *J. Phys. Chem.* **1981**, *85*, 7.
20 C. Reylé, P. Bréchignac, *Eur. Phys. J. D* **2000**, *8*, 205.
21 M. Misono, J. Wang, M. Ushino, M. Okubo, H. Katô, M. Baba, S. Nagakura, *J. Chem. Phys.* **2002**, *116*, 162.
22 A. Doi, S. Kasahara, H. Katô, M. Baba, *J. Chem. Phys.* **2004**, *120*, 6439.
23 J. Wang, A. Doi, S. Kasahara, H. Katô, M. Baba, *J. Chem. Phys.* **2004**, *121*, 9188.
24 D. Y. Baek, J. Wang, A. Doi, S. Kasahara, H. Katô, M. Baba, *J. Phys. Chem. A* **2005**, *109*, 7127.
25 D. Y. Baek, J. Chen, J. Wang, A. Doi, S. Kasahara, M. Baba, H. Katô, *Bull. Chem. Soc. Jpn.* **2006**, *79*, 75.
26 M. Okubo, M. Misono, J. Wang, M. Baba, H. Katô, *J. Chem. Phys.* **2002**, *116*, 9293.
27 D. L. Joo, R. Takahashi, J. O'Reilly, H. Katô, M. Baba, *J. Mol. Spectrosc.* **2002**, *215*, 155.
28 M. Okubo, J. Wang, M. Baba, M. Misono, S. Kasahara, H. Katô, *J. Chem. Phys.* **2005**, *122*, 144303.
29 W. Demtröder, *Laser Spectroscopy*, Springer-Verlag, Berlin, **1981**.
30 E. Riedle, H. J. Neusser, E. W. Schlag, *J. Chem. Phys.* **1981**, *75*, 4231.
31 A. Doi, M. Baba, S. Kasahara, H. Katô, *J. Mol. Spectrosc.* **2004**, *227*, 180.
32 M. H. Kabir, S. Kasahara, W. Demtröder, Y. Tatamitani, M. Okubo, M. Misono, J. Wang, M. Baba, D. L. Joo, J. O'Reilly, A. Doi, Y. Kimura, H. Katô, *Chem. Phys.* **2002**, *283*, 237.
33 M. H. Kabir, S. Kasahara, W. Demtröder, Y. Tatamitani, A. Doi, H. Katô, M. Baba, *J. Chem. Phys.* **2003**, *119*, 3691.
34 H. Katô, *Bull. Chem. Soc. Jpn.* **1993**, *66*, 3203.
35 F. Metz, W. E. Howard, L. Wunsch, H. J. Neusser, E. W. Schlag, *Proc. R. Soc. London, Ser. A* **1978**, *363*, 381.
36 E. Riedle, H. J. Neusser, E. W. Schlag, *J. Phys. Chem.* **1982**, *86*, 4847.
37 E. Riedle, H. J. Neusser, *J. Chem. Phys.* **1984**, *80*, 4686.
38 U. Schubert, E. Riedle, H. J. Neusser, E. W. Schlag, *Isr. J. Chem.* **1990**, *30*, 197.
39 N. Nakashima, K. Yoshihara, *J. Chem. Phys.* **1982**, *77*, 6040.
40 R. Pariser, *J. Chem. Phys.* **1956**, *24*, 250.
41 G. Herzberg, *Molecular Spectra and Molecular Structure. II. Infrared and Raman Spectra of Polyatomic Molecules*, Van Nostrand Reinhold, New York, **1945**.
42 C. W. Ashpole, S. J. Formosinho, G. Porter, *Proc. R. Soc. London, Ser. A* **1971**, *323*, 11.
43 H. Schröder, H. J. Neusser, E. W. Schlag, *Chem. Phys. Lett.* **1978**, *54*, 4.

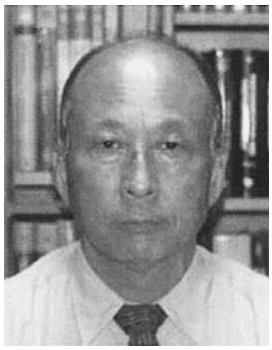

Hajime Katô was born in Gifu, Japan, in 1941. After his B.S. and M.A. studies at the Faculty of Science, Kyoto University and his Ph.D. studies at the Faculty of Engineering, Kyoto University (the supervisors were Professor T. Yamamoto and T. Yonezawa, respectively), he moved to the Faculty of Science, Kobe University as a research associate in 1968. He received degree of D.S. in 1972 from Kyoto University by studies on the MCD spectra of transition-metal complexes. He was attracted to the beautiful world of high resolution laser spectroscopy during studies in U.K. as a Japanese Ramsay fellow (1973.9–1975.8). His research had been focused on studies of molecular structure and dynamics by developing various techniques of high-resolution laser spectroscopy in visible and U.V. region. He was promoted to a professor of Kobe University in 1985 and an emeritus professor of Kobe University in 2005.

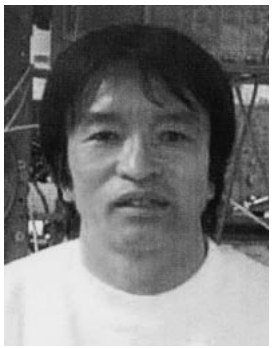

Masaaki Baba was born in 1955 in Fukuoka, Japan. He graduated from Kyoto University in 1977, and received his D.Sc. there in 1985 under the supervision of Professor Noboru Hirota. He joined the research group of Professor Ichiro Hanazaki in the Institute for Molecular Science as a technical associate, and began the work on laser spectroscopy using the molecular beam technique. In 1986, he moved as a research associate of Professor Hajime Katô to Faculty of Science, Kobe University. Since then, he has been concerned with high-resolution molecular spectroscopy. His research interests include the molecular structure and excited-state dynamics of polyatomic molecules. Now he is an Associate Professor at the Faculty of Science, Kyoto University.

Shunji Kasahara was born in Toyooka, Japan in 1965. He received his B.S. degree in 1988, and his doctor degree in 1993 from Kobe University under the supervision of Prof. Katô. In 1993, he became Research Associate of the Graduate School of Science and Technology of Kobe University. In 1996, he became Research Associate of the Department of Chemistry of Kobe University. Since 2001, he has been Associate Professor of the Molecular Photoscience Research Center, Kobe University. His current research interests are studies of excited molecules through the rotationally resolved high-resolution laser spectroscopy.